

Chlorine–Oxygen Interactions and the Role of Chlorine in Ethylene Oxidation over Ag(111)

S. A. TAN, R. B. GRANT,¹ AND R. M. LAMBERT²

Department of Physical Chemistry, University of Cambridge, Cambridge CB2 1EP, England

Received November 25, 1985; revised February 24, 1986

Coadsorbed chlorine enhances the surface \rightarrow bulk transport of chemisorbed oxygen on Ag(111). Preadsorbed chlorine progressively blocks the chemisorption of atomic oxygen (O(a)); O(a) uptake is completely suppressed at $\theta_{\text{Cl}} = 0.25$. Reactor studies of ethylene oxidation in the presence of adsorbed chlorine show that Cl reduces overall activity and increases selectivity towards ethylene oxide formation. All catalytic activity is quenched for chlorine fractional coverages ≥ 0.25 . This strongly suggests that O(a) is the crucial surface species responsible for both selective and total oxidation of ethylene. Temperature-programmed reaction data indicate that under certain conditions Cl exerts an apparent antipromoter effect. The relevant conditions are remote from those which prevail in a typical flow reactor. © 1986 Academic Press, Inc.

INTRODUCTION

The molecular pathway by which ethylene is catalytically oxidised to ethylene oxide (EO) over Ag and the role of chlorine as a selectivity promoter in this process are still matters for debate. The subject has been extensively reviewed (1–5) and much discussion centres on the identity of the epoxidising surface species. Is it chemisorbed atomic oxygen (O(a)) or chemisorbed dioxygen (O₂(a))? The latter hypothesis gained considerable favour following work by Sachtler and co-workers (1, 6); a number of laboratories have subsequently produced results which, with varying degrees of directness, have been interpreted in favour of the dioxygen hypothesis (7–10). Some of this work has involved investigating the effect of Cl on reaction selectivity (1, 6, 11).

However, yet other results, obtained by essentially similar experimental approaches, have been taken to support the

atomic oxygen hypothesis (12–15). Again, experiments involving chlorine have played a part (16, 17). Most recently, work on Ag powders (18) and on Ag(111) (19, 20) has indicated that O(a) is the epoxidising agent. Following our earlier single crystal investigations of ethylene oxidation, ethylene oxide isomerisation, and the role of Cs in these systems, we report here on the interaction of chlorine and oxygen on Ag(111) and on the influence of chlorine on the oxidation chemistry of ethylene under batch reactor and temperature-programmed reaction (TPR) conditions.

METHODS

The apparatus consisted of an ultrahigh vacuum spectrometer chamber coupled directly to a high-pressure reactor cell. The UHV chamber was equipped with the usual facilities for LEED/Auger analysis and Ar⁺ etching. It also contained a quadrupole mass spectrometer allowing temperature-programmed thermal desorption spectra to be recorded. The specimen could be rapidly transferred between the UHV chamber and a 75-ml reactor via a special gate valve; reactant and product partial pressures and

¹ Present address: VG Gas Analysis Ltd, Nat Lane, Winsford, Cheshire CW7 3QH, England.

² To whom correspondence should be addressed.

their time dependence were monitored by a second quadrupole mass spectrometer sampling through a variable leak valve. Transfer time in the reverse direction from about 10 to $\sim 10^{-9}$ Torr could typically be achieved within 60 s: surface analysis could therefore be carried out both immediately before and immediately after catalytic runs in the pressure cell which was operated as a differential batch reactor. Exposures are quoted in Langmuirs (1 Langmuir = 1 L = 10^{-6} Torr s).

The 99.999% purity (111)-oriented Ag specimen was prepared as a thin wafer (0.6 mm thick, 8.6 mm diameter) in order to obtain a favourable ratio of (111) face area to edge area (7 : 1). Furthermore, the specimen manipulator permitted preparation, examination and doping of *both* (111) crystal faces so that structural and chemical characterisation of the entire active surface area was achieved. Precision dosing of *both* faces with chlorine was carried out by means of an electrochemically generated molecular beam of Cl_2 . The construction of this feedback-controlled AgCl electrolysis cell has been described elsewhere (21) and chlorine fractional coverages are referred to the number density of metal atoms in the (111) plane. Research grade O_2 and C_2H_4 were used throughout the work, and Cs dosing was achieved with a collimated commercial thermal evaporation source (SAES Getters). Conversion levels in the reactor correspond to $\leq 2\%$ of the initial ethylene.

RESULTS

Chemisorption of Chlorine and Oxygen

LEED and Auger spectroscopy were used to monitor uptake of chlorine by the clean (111) surface at 300 K. The initial sticking probability of Cl_2 was ~ 0.3 and upon saturation the formation of a (10×10) overlayer structure was seen, corresponding to $\theta_{\text{Cl}} = 0.49$ (Fig. 3), both observations being in good agreement with earlier work (22, 23). In subsequent TPD measurements (heating rate $\sim 11 \text{ K s}^{-1}$) the chlorine overlayer evaporated as AgCl

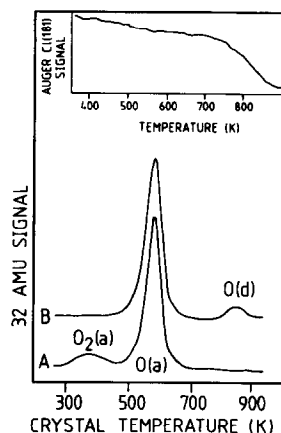


FIG. 1. Oxygen desorption spectra after 300 K exposure to 6×10^7 L of O_2 at 2 Torr pressure. (A) Clean surface. (B) In the presence of a high level of lattice oxygen. Inset shows temperature dependence of C1 Auger signal in the absence of oxygen obtained in a separate experiment (see text).

yielding a desorption peak at ~ 870 K. This is in line with the observations of Bowker and Waugh (22) for the Ag(111)- Cl_2 system. Saturating the initially clean surface with oxygen at 300 K and 2 Torr gave rise to TPD spectra which exhibited two peaks at 380 K and 580 K (Fig. 1A) which are assigned, respectively, to $\text{O}_2(\text{a})$ and $\text{O}(\text{a})$, as reported previously (24). Repeating such adsorption/desorption cycles did not significantly increase the amount of oxygen incorporated into the Ag lattice: Auger spectroscopy revealed that the $\text{O}(515 \text{ eV})/\text{Ag}(356 \text{ eV})$ intensity ratio was always $\leq 2\%$. However, *coadsorption* of chlorine and oxygen was found to markedly affect the surface \rightarrow bulk transport of chemisorbed oxygen. Thus repeated cycles of chlorine preadsorption ($\theta_{\text{Cl}} \approx 0.1$) followed by saturation dosing with oxygen (300 K, 2 Torr) and desorption resulted in a progressive increase of the above Auger intensity ratio to a limiting value of $\sim 6.2\%$. This strongly suggests that the presence of $\text{Cl}(\text{a})$ can induce substantial amounts of $\text{O}(\text{a})$ to dissolve in the bulk metal. The nature of this lattice-incorporated oxygen was further revealed by its desorption characteristics and its Auger

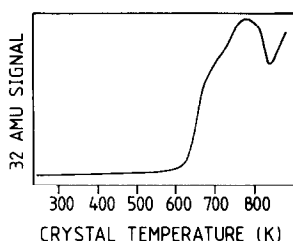


FIG. 2. Extraction of lattice oxygen by chemisorbed Cs. O_2 desorption spectrum after dosing with 0.2 monolayers of Cs (no O(a) present).

spectrum: it was found to evaporate only at temperatures in excess of 900 K, at which point the evaporation rate of the Ag lattice itself becomes appreciable. When the nominally clean surface (i.e., with no adsorbed species but containing a high level of bulk oxygen) was saturated with surface oxygen (2 Torr, 300 K), the oxygen:Ag Auger intensity ratio was found to be $\sim 9.1\%$ and a kinetic energy shift in the oxygen Auger signal was observed. While the Auger electron kinetic energy for bulk oxygen was measured to be 515 eV, that for surface oxygen was observed at 525 eV. The presence of high levels of bulk oxygen beneath an otherwise nominally clean surface (i.e., one which desorbed no oxygen below 900 K) was also proved by dosing such a surface with ~ 0.2 monolayers of Cs and performing a TPD sweep. Oxygen desorption then occurs in a complex fashion (Fig. 2) indicating that Cs(a) causes bulk oxygen to diffuse back to the surface. Cs itself does not diffuse into Ag under these conditions (19) and these complex oxygen desorption spectra are assigned to the decomposition of a Cs/O surface phase (19).

High-pressure oxygen chemisorption on the oxygen-loaded specimen (i.e., in the presence of high levels of lattice oxygen) resulted in a very pronounced change in the subsequent O_2 desorption behavior (Fig. 1B) as compared with the clean crystal case. The 380 K peak due to $O_2(a)$ is seen to be absent while a new peak has appeared at ~ 850 K. This latter is assigned to the desorption of subsurface or dissolved oxygen

and the corresponding species will be designated O(d). Its appearance in thermal desorption has previously only been reported following low pressure oxygen dosing of Ag single crystals containing significant amounts of dissolved alkali (25, 26). The present observation would appear to be the first time that room-temperature oxygen dosing has resulted in the detection of this high-temperature O(d) desorption feature from alkali-free single crystal Ag.

Coadsorption experiments with chlorine and oxygen were carried out on this surface (i.e., with a high level of lattice oxygen) which will later be shown to be catalytically active for the selective oxidation of ethylene. The blocking of oxygen chemisorption by preadsorbed chlorine is illustrated in Fig. 3A which shows the effect of varying precoverages of Cl on the subsequent saturation uptake of oxygen at 300 K and 2 Torr pressure. Oxygen uptake was measured by means of the O_2 thermal desorption yield while chlorine coverages were monitored by Auger spectroscopy. It can be seen that preadsorbed chlorine blocks both O(a) chemisorption and O(d) uptake at a coverage of $\theta_{Cl} = 0.25$; Auger spectroscopy confirmed that there was no displacement of chlorine by oxygen under these conditions. Similar results for O(a) blocking by preadsorbed Cl have been reported for Ag(100) (26),

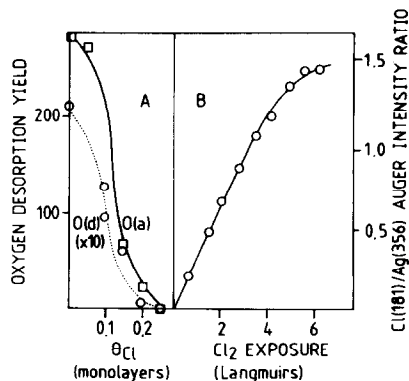


FIG. 3. (A) Effect of Cl precoverage on uptake of O(a) and O(d). (B) Chlorine uptake at 300 K monitored by Auger spectroscopy.

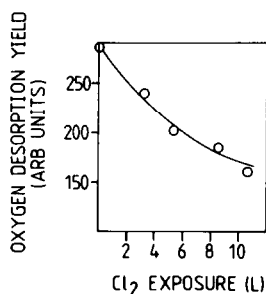


FIG. 4. Displacement of preadsorbed oxygen by chlorine at 300 K.

Ag(110) (27), and Ag powders (1). It thus appears that $\theta_{\text{Cl}} \sim 0.25$ represents a critical coverage on any low index or polycrystalline Ag surface above which the chemisorption of O(a) is effectively suppressed. The converse experiments, i.e., presaturation with oxygen at 2 Torr followed by varying exposures to chlorine indicate that O(a) is removed from the surface by Cl(a) (Fig. 4). In addition, increasingly complex features appear in the oxygen desorption spectra between 580 and 850 K as a function of increasing chlorine exposure (Fig. 5). These features are characteristic of oxygen species desorbing from the bulk and near sub-surface regions of the crystal (28); their appearance confirms the observation that surface \rightarrow bulk diffusion of oxygen is enhanced by the presence of chlorine.

Effect of Chlorine on Ethylene Oxidation: TPR Observations

With a high level of bulk oxygen in the sample, temperature-programmed reaction

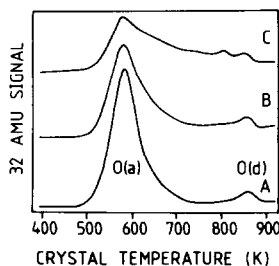


FIG. 5. O₂ desorption spectra showing Cl-enhanced dissolution of oxygen. A, B, and C correspond to Cl₂ exposures of 2.7, 5.4, and 8.0 L, respectively.

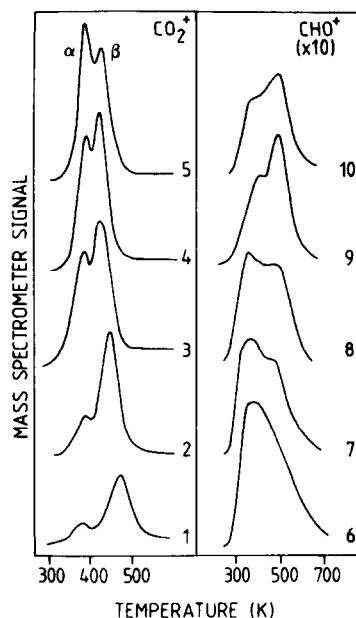


FIG. 6. TPR spectra as a function of C₂H₄ exposure from the oxygen presaturated surface. 1, 2, 3, 4, and 5 correspond to 1.2×10^6 , 7.5×10^6 , 15×10^6 , 30×10^6 , and 45×10^6 L of C₂H₄, respectively, while 6, 7, 8, 9, and 10 correspond to 1.2×10^6 , 3×10^6 , 9×10^6 , 13.5×10^6 , and 22.5×10^6 L of C₂H₄, respectively.

measurements were carried out in order to investigate certain aspects of the system's reactive behaviour under Langmuir-Hinshelwood conditions with high initial coverages of reactants and effectively 100% conversion to products. In one series of experiments the Cl-free surface was presaturated with oxygen (2 Torr, 300 K) and then subjected to varying doses of ethylene at 300 K. A TPR sweep was then performed ($\sim 11 \text{ K s}^{-1}$) while monitoring the CO₂ and ethylene oxide yields at 44 and 29 a.m.u., respectively, (the contribution of C₂H₄O⁺ to the 44-a.m.u. signal is negligible under these conditions (29)). Typical results are shown in Fig. 6; the α and β CO₂ peaks result from the direct combustion of ethylene and from the further oxidation of ethylene oxide, respectively (20). Curve A of Fig. 7 shows that the α : β peak area ratio increases with increasing ethylene dose (i.e., ethylene coverage), while a corresponding decrease occurs in the 29-a.m.u.

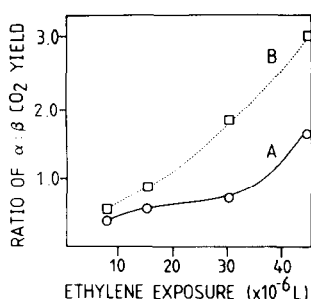


FIG. 7. TPR data showing effect of ethylene exposure on $\alpha:\beta$ CO_2 ratio from an oxygen presaturated surface. (A) Chlorine-free surface. (B) $\theta_{\text{Cl}} = 0.063$.

CHO^+ desorption yield from ethylene oxide and acetaldehyde (Fig. 6); the latter has been previously shown to arise from the isomerisation of ethylene oxide (20, 30). Predosing the surface with chlorine before such TPR measurements caused no change in the shapes or temperatures of the α and β CO_2 peaks, but did cause a systematic increase in the $\alpha:\beta$ CO_2 ratio. Curve B of Fig. 7 illustrates this effect of Cl as a function of ethylene coverage for $\theta_{\text{Cl}} = 0.063$. Thus under these TPR conditions, preadsorbed chlorine appears to *increase* the relative amount of C_2H_4 which is directly oxidised to $\text{CO}_2 + \text{H}_2\text{O}$. Note that this is in contradistinction with what one expects under normal catalytic conditions (~ 500 K and elevated pressures).

This behaviour was investigated further by examining the response of the system as a function of chlorine precoverage for fixed doses of oxygen and ethylene. Figure 8A shows TPR results for the θ_{Cl} dependence of the $\alpha:\beta$ CO_2 ratio, the residual (unreacted) O(a) thermal desorption yield and the 29-a.m.u. CHO^+ yield for an oxygen-saturated surface dosed with 8×10^5 L of C_2H_4 ($\theta_{\text{C}_2\text{H}_4} \sim 0.004$). Parts B and C of Fig. 8 show similar data for successively larger ethylene coverages: $\theta_{\text{C}_2\text{H}_4} \sim 0.024$ and ~ 0.045 , respectively. (The ethylene coverage is calculated from a knowledge of the CO_2 desorption yield, the latter being calibrated with respect to the O_2 desorption yield associated with a known LEED struc-

ture (24)). From this set of experiments it is clear that the $\alpha:\beta$ CO_2 ratio is a particularly sensitive function of the initial ethylene coverage; the EO yield also shows a systematic dependence on θ_{Cl} .

Reactor Studies of the Effect of Chlorine on Ethylene Oxidation

Reactor studies were carried out with the crystal surface prepared in the same manner as for the above TPR measurements. Chlorine was preadsorbed to varying coverages prior to running the reaction at 550 K in a 2:1 mixture of ethylene: oxygen at a total pressure of 6 Torr, and the results are shown in Figs. 9A–C. Auger spectroscopy showed that there was no loss of Cl(a) during these measurements, and the latter may be summarised as follows:

1. Increasing θ_{Cl} leads to a monotonic decrease in CO_2 activity which results in a monotonic increase in selectivity towards EO.
2. Both EO and CO_2 activities tend to zero at $\theta_{\text{Cl}} = 0.25$; this is the chlorine coverage at which the uptakes of both O(a) and O(d) are completely suppressed at this same oxygen partial pressure. (The small residual activity at $\theta_{\text{Cl}} = 0.25$ which is just apparent in Fig. 9A can be accounted for by

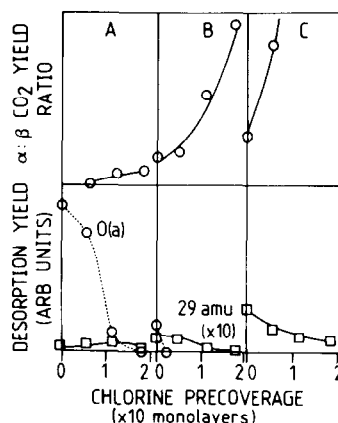


FIG. 8. Effect of Cl precoverage on TPR O(a) , 29 a.m.u. yields and $\alpha:\beta$ CO_2 ratio for the oxygen saturated surface. A, B, and C refer to ethylene exposures of 8.0×10^5 , 7.5×10^6 , and 6.0×10^7 L, respectively.

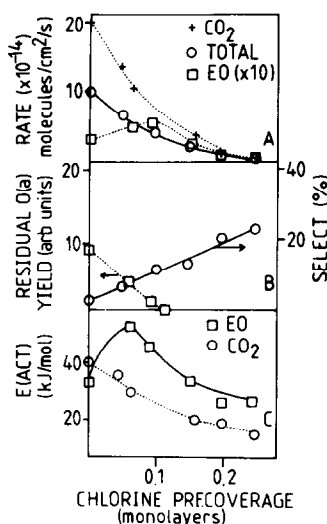


FIG. 9. Reactor data showing effect of Cl precoverage. (A) Turnover frequencies. (B) Selectivity and post-reactor O(a) desorption yield. (C) Activation energies.

residual reaction at the specimen edges which could not be uniformly dosed with Cl_2 as were the back and front (111) faces).

3. Apparent activation energies show a generally decreasing trend.

4. Post-reactor measurements of the residual O(a) TDS yield (Fig. 8B) do *not* correlate quantitatively with the point at which O(a) blocking is complete (i.e., $\theta_{\text{Cl}} = 0.25$). The postreactor O(a) TDS yield cuts off at $0.09 \leq \theta_{\text{Cl}} \leq 0.15$.

Control experiments showed that such measurements provide only a *qualitative* indication of the amount of O(a) present on the surface under reaction conditions. The discrepancy arises because some O(a) is lost from the surface by reaction and diffusion during the pump-down and specimen transfer procedure. During the cooling and pump-down phase some ethylene necessarily coadsorbs with O(a); this undergoes oxidation (mainly to CO_2) both at this stage and during the subsequent TDS measurement. The CO_2 yield observed in the TDS measurement is of the order of the O_2 yield and depends on the particular procedure adopted for specimen transfer. This CO_2 yield cannot be used to obtain a value for

O(a) corrected for post-reactor oxidation reactions because an unknown (and variable) amount of CO_2 is lost in the reactor cell before the TDS measurement can be carried out.

DISCUSSION

Oxygen Uptake by Silver in the Presence of Chlorine

The ability of preadsorbed chlorine to inhibit the subsequent chemisorption of O(a) has previously been reported on a range of Ag surfaces including supported, polycrystalline and single crystal specimens both in the absence and in the presence of surface alkali (1, 6, 11, 26, 27, 31). We now report, for the first time, essentially quantitatively identical behaviour on the (111) face. The point is of some significance because (111) faces are likely to predominate at the surfaces of practical Ag catalysts. It now also appears that the presence of Cl facilitates the diffusion of oxygen into Ag (Figs. 1B and 5). This enhancement may result from the chlorine-induced reaction of $\text{Ag}^{\delta+}$ sites such that the contracted atomic size of the metal permits easier transport of oxygen. The tendency of Cl itself to diffuse into Ag at modest temperatures would appear to lend credence to this view. This behaviour is illustrated in the inset to Fig. 1 which shows the temperature dependence of the Cl Auger intensity from the clean Ag surface precovered to $\theta_{\text{Cl}} = 0.25$.

For chlorine loadings in excess of one monolayer, Bowker and Waugh (22, 32) have observed efficient surface \rightarrow bulk transport of Cl on single crystal Ag(111) and Ag(110) at relatively low temperatures. Chlorine-induced oxygen loading of Ag can evidently lead to a situation in which a distinct peak due to subsurface oxygen eventually appears in the O_2 desorption spectra (Fig. 1A). This subsurface oxygen desorption peak resembles in some respects the high-temperature desorption feature which develops when Ag(110) is subjected to plasma-induced oxidation in a low-pressure oxygen discharge (28); in that work it was

also suggested that the high-temperature O_2 peak was due to O(d). The ability of a sufficiently high level of lattice oxygen to suppress the chemisorption of $O_2(a)$ (Fig. 1B) is at least consistent with the observation (25, 33) that dissolved alkali enhances the adsorption of $O_2(a)$. One might speculate that in the present case, lowering of the local work function by lattice oxygen increases charge donation into the π^* orbital of $O_2(a)$ and hence favours dissociation of the latter species. The observed 10-eV kinetic energy difference between the *KLL* Auger signals for O(a) and lattice oxygen can adequately be accounted for in terms of the difference in 2-hole extra-atomic relaxation energies for the two oxygen species (34, 35) if one considers the lattice oxygen to be in an essentially oxide-like environment. Such relaxation effects generally swamp the much smaller differences reported for the O(1s) core-level binding energy shifts between O(a) on Ag and lattice oxygen in Ag_2O (36). Finally the ability of chlorine to displace preadsorbed O(a) may be used to obtain an estimate of the Ag–Cl chemisorption bond strength. In the case of Ag(111) the Ag–O bond energy is ~ 314 kJ/mol (24); if the displacement reaction is $Cl_2(g) + 2O(a) \rightarrow 2Cl(a) + O_2(g)$, then $\Delta H \leq 0$ and given the dissociation energy of $Cl_2(g)$ it follows that the strength of the Ag–Cl chemisorption bond is ≥ 186 kJ/mol.

Oxidation of Ethylene in the Presence of Chlorine

The reactor results illustrated in Fig. 9A are of central importance. They demonstrate that *all* oxidation activity, both total and partial, ceases at $\theta_{Cl} = 0.25$ at which point the surface is completely blocked to O(a) chemisorption. (Recall that Cl(a) is not displaced by oxygen and that Auger spectroscopy shows no Cl depletion under reaction conditions.) This observation provides strong support for the view that O(a) is the crucial surface species which leads both to EO formation and to ethylene combustion. In an earlier paper (19), we reached the same conclusion on the basis of quite differ-

ent evidence. More recently, van Santen and de Groot have used ^{18}O labelling experiments with Ag powder catalysts in the absence of Cl to demonstrate directly that O(a) is the selective oxidant (18). In the present case, note that if one uses the post-reactor O_2 desorption yield (Fig. 9B) as a *quantitative indication* of the O(a) coverage under reaction conditions, then the opposite conclusion is reached: namely that O(a) is not the only oxidising species in the system. As already pointed out, this would not be a valid procedure in our apparatus. A very similar procedure *has* been used and interpreted quantitatively in favour of the $O_2(a)$ hypothesis, i.e., that O(a) is not responsible for partial oxidation (27). Such a view appears to be increasingly hard to sustain in the light of the present results and the results of van Santen and de Groot (18). The decrease in apparent activation energies for both EO and CO_2 formation which occurs at higher chlorine coverages has been reported previously (11) and may be similarly rationalised: as θ_{Cl} becomes sufficiently great ethylene adsorption becomes rate-determining.

In an earlier paper (20) we argued that the role of Cl as a promoter under the usual reaction conditions can be rationalised in terms of the way in which it alters the amount of valence charge on O(a). By competing for and thus decreasing the amount of negative charge on O(a), adsorbed chlorine favours electrophilic attack by ethylene on O(a) (leading to EO formation) and disfavors H-stripping by O(a) (which would lead to combustion). With this in mind, it is of interest to consider the TPR data in Fig. 8. Recall that these experiments represent 100% conversion of the adsorbed ethylene under nonisothermal conditions. They cannot therefore be compared very directly with the batch reactor data. Nevertheless, interesting trends are discernible. At low ethylene coverages ($\theta_{C_2H_4} \sim 0.004$, Fig. 8A) the system crudely mimics the behaviour in the reactor: with increasing θ_{Cl} there is some increase in the EO yield while the $\alpha:\beta$ CO_2 ratio is relatively little af-

fect. With successively larger doses of ethylene, essentially contrary behaviour sets in (Figs. 8B,C). Increased θ_{Cl} now results in a definite decrease in the EO yield and a very marked increase in the $\alpha : \beta$ CO_2 yield; both responses correspond to a significant *decrease* in selectivity. The important difference, however, is that we are now dealing with much greater ethylene precoverages ($\theta_{\text{C}_2\text{H}_4} \sim 0.024$ to ~ 0.045) and ethylene is an electron donor. Its effect on the charge state of O(a) will be opposite to that of Cl. Given that Cl(a) can enhance ethylene adsorption on Ag(110) (27) the following explanation may be offered. At high ethylene doses, an important effect of Cl(a) is to significantly increase the uptake of ethylene. The resulting increase in charge donation from the hydrocarbon-rich layer then renders the O(a) less selective, by the argument developed above. If correct, this interpretation would be consistent with the view that in a catalytic reactor at elevated temperatures of ~ 500 K the steady-state population of weakly bound $\text{C}_2\text{H}_4(\text{a})$ is very small. The charge state of O(a) is therefore controlled by the relatively large coverage of strongly bound Cl(a) which in consequence exercises its "normal" promoter effect.

Given this essentially "electronic" explanation for the promoter effect due to chlorine, one might ask how it is that alkalis can also have a favourable effect on selectivity. We have dealt with this point in earlier publications (19, 20, 30). The hypothesis is that the predominant effect of Cl is on the primary chemistry ($\text{C}_2\text{H}_4 \rightarrow \text{EO}$ versus CO_2) whereas alkalis act principally on the secondary chemistry by inhibiting the Ag-catalysed isomerisation of ethylene oxide, a reaction which would otherwise lead to rapid burning of the product ($\text{EO} \rightarrow \text{CH}_3\text{CHO} \rightarrow \text{CO}_2$). That this explanation is at least consistent is indicated by the observations that Cs *disfavours* selectivity in the primary chemistry and that Cl *enhances* the Ag-catalysed isomerization of ethylene oxide (37).

CONCLUSIONS

1. Coadsorbed chlorine enhances surface \rightarrow bulk transport of O(a) on Ag(111). This subsurface oxygen can be recognised by a characteristic thermal desorption peak and by Auger spectroscopy.

2. Chlorine can displace preadsorbed O(a) even at 300 K. However, preadsorbed Cl is unaffected by oxygen dosing and can completely block the surface to O(a) chemisorption when $\theta_{\text{Cl}} \geq 0.25$.

3. Reactor data exhibit the expected fall in activity and increase in selectivity with increasing θ_{Cl} . When $\theta_{\text{Cl}} = 0.25$ both partial and total oxidation reactions cease. Therefore O(a) is the oxidant for both types of chemistry. In our apparatus, postreactor measurements of the O_2 thermal desorption yield do not provide a quantitative measure of the O(a) coverage under reaction conditions.

4. Temperature-programmed reaction data suggest that the "normal" promoter effect of chlorine depends on there being present only a very low coverage of ethylene. At high ethylene coverages, Cl can exhibit an antipromoter effect in the TPR mode.

ACKNOWLEDGMENT

We are grateful to Johnson Matthey Ltd. for a loan of precious metals.

REFERENCES

1. Kilty, P. A., and Sachtler, W. M. H., *Catal. Rev.-Sci. Eng.* **10**, 1 (1974).
2. Sachtler, W. M. H., Backx, C., and van Santen, R. A., *Catal. Rev.-Sci. Eng.* **23**, 127 (1981).
3. Clayton, R. W., *Chem. Soc. Spec. Period. Rep.-Catal.* **3**, 70 (1980).
4. Hucknell, D. J., "Selective Oxidation of Hydrocarbons," Chap. 2. Academic Press, New York, 1974.
5. Verykios, X. E., Stern, F. P., and Coughlin, R. W., *Catal. Rev.-Sci. Eng.* **22**, 197 (1980).
6. Kilty, P. A., Rol, N. C., and Sachtler, W. M. H., in "Proceedings, 5th International Congress on Catalysis, Palm Beach, 1972" (J. W. Hightower, Ed.), p. 929. North-Holland, Amsterdam, 1973.
7. Cant, N. K., and Hall, W. K., *J. Catal.* **52**, 81 (1978).

8. Stoukidas, N., and Vayenas, C. G., *J. Catal.* **69**, 18 (1981).
9. Akimoto, M., Ichikawa, I., and Echigoya, E., *J. Catal.* **76**, 333 (1982).
10. Kenson, K. E., and Lapkin, M. J., *J. Phys. Chem.* **74**, 1493 (1970).
11. Campbell, C. T., and Koel, B. E., *J. Catal.* **92**, 272 (1985).
12. Force, E. L., and Bell, A. T., *J. Catal.* **38**, 440 (1975).
13. Force, E. L., and Bell, A. T., *J. Catal.* **40**, 356 (1975).
14. Haul, R., Hoge, D., Neubauer, G., and Zeeck, U., *Surf. Sci.* **122**, L622 (1982).
15. Backx, C., Moolhuysen, J., Geenen, P., and van Santen, R. A., *J. Catal.* **72**, 364 (1981).
16. Force, E. L., and Bell, A. T., *J. Catal.* **44**, 175 (1976).
17. van Santen, R. A., Moolhuysen, J., and Sachtler, W. M. H., *J. Catal.* **65**, 478 (1980).
18. van Santen, R. A., and de Groot, C. P. M., in press.
19. Grant, R. B., and Lambert, R. M., *Langmuir* **1**, 29 (1985).
20. Grant, R. B., and Lambert, R. M., *J. Catal.* **92**, 364 (1985).
21. Spencer, N. D., Goddard, P. J., Davies, P. W., Kitson, M., and Lambert, R. M., *J. Vac. Sci. Technol.* **A1**, 1554 (1983).
22. Bowker, M., and Waugh, K. C., *Surf. Sci.* **134**, 639 (1983).
23. Goddard, P. J., and Lambert R. M., *Surf. Sci.* **67**, 180 (1977).
24. Grant, R. B., and Lambert, R. M., *Surf. Sci.* **146**, 256 (1984).
25. Kitson, M., and Lambert, R. M., *Surf. Sci.* **109**, 60 (1981).
26. Kitson, M., Ph.D. thesis. University of Cambridge, August 1980.
27. Campbell, C. T., and Paffett, M. T., *Appl. Surf. Sci.* **19**, 28 (1983).
28. Bowker, M., *Surf. Sci.* **155**, L276 (1985).
29. Cornu, A., and Massot, R., "Compilation of Mass Spectrometer Data." Heyden, London, 1979.
30. Grant, R. B., and Lambert, R. M., *J. Catal.* **93**, 92 (1985).
31. Au, C. T., Boparai, S. S., Roberts, M. W., and Joyner, R. W., *J. Chem. Soc. Faraday Trans. 1* **79**, 1779 (1983).
32. Bowker, M., and Waugh, K. C., *Surf. Sci.* **155**, 1 (1985).
33. Spencer, N. D., and Lambert, R. M., *Chem. Phys. Lett.* **83**, 388 (1981).
34. Fuggle, J. C., in "Electron Spectroscopy Theory, Techniques and Applications" (C. R. Brundle and A. D. Baker, Eds.), Vol. 4, p. 86. Academic Press, New York, 1981.
35. Joyner, R. W., and Roberts, M. W., *Chem. Soc. Spec. Period. Rep.* **4**, 68 (1975).
36. Schön, G., *Acta Chem. Scand.* **27**, 2623 (1973).
37. Tan, S. A., and Lambert, R. M., in preparation.